XXI IMEKO World Congress "Measurement in Research and Industry"
August 30 – September 4, 2015, Prague, Czech Republic

ANALYSIS OF PRESSURE DISTRIBUTION ON THE SONDA III VEHICLE IN TRANSONIC REGIME

M. L. C. C. Reis [1], *J. B. P. F. Filho* [2], *E. Basso* [3], *J. D. Costa* [4]
[1,2,3] Instituto de Aeronáutica e Espaço, São José dos Campos, Brazil
marialuisamlccr@iae.cta.br, jb.falcao@ig.com.br, edsonbasso@iae.cta.br
[4] Faculdade de Tecnologia Prof. Jessen Vidal, São José dos Campos, Brazil, dorcejonathan@gmail.com

Abstract – A half model of the aerospace vehicle Sonda III is being tested at the Brazilian Pilot Transonic Wind Tunnel. The aim of the tests is to study the presence of shock and expansion waves in the inter-stage region of the vehicle. Special emphasis is placed on the nominal Mach number 0.90. Measured values are static pressure on the model surface and freestream total and static pressures. The estimated parameters are pressure coefficients and Mach number. Numerical analysis of the flow field parameters is done and compared to experimental results.

Keywords: Shock waves, Uncertainty in measurements, Sounding rocket, Transonic wind tunnel

1. INTRODUCTION

In this study, we analyse the pressure and Mach number distribution on the surface of the aerospace vehicle Sonda III. The sounding rocket family named Sonda was conceived and produced by the Brazilian Institute of Aeronautics and Space. The project started in the 1960's and a prototype of Sonda I was launched in 1967, at the Barreira do Inferno rocket launch centre. Sonda III was developed for validation of technological innovations such as stage separation, second stage ignition and tele-destruction. It was launched 31 times and its first flight occurred in 1976. The Sonda series has been gradually developed up to the VS-40 vehicle with a view to dominating critical technologies for the construction of the Satellite Launch Vehicle, VLS (Fig. 1).

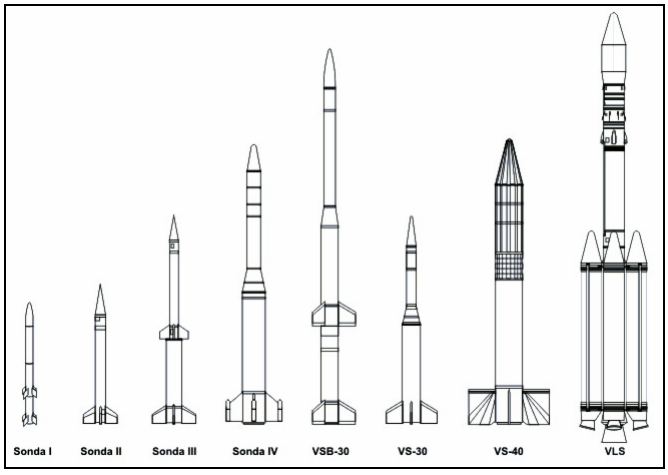

Fig. 1. Brazilian sounding rockets and the Satellite Launch Vehicle.

A half model of the Sonda III vehicle is being tested at the Pilot Transonic Wind Tunnel of the Aerodynamics Division of the Institute of Aeronautics and Space, IAE/ALA/TTP (Fig. 2).

Fig. 2. The Pilot Transonic Wind Tunnel circuitry.

The purpose of the test campaign is to verify aerodynamic phenomena in the airflow around the vehicle which can compromise its flight performance.

In the presence of shock and expansion waves, the flow field parameters static temperature, T, density, ρ, static pressure, p, and velocity, V, change significantly [1]. After passing a shock wave, airflow velocity decreases while density, static temperature and static pressure increase. If expansion waves occur, the opposite behaviour is observed.

The campaign started with a flat plate model in order to verify the metrological reliability in studying shock and expansion waves at the TTP facility [2].

The Sonda III half model has two stages linked by the inter-stage region in a frustum cone shape. It has three basic configurations: no fins, with a single fin positioned at 90° in relation to the longitudinal axis of the fuselage, as shown in Fig. 3, and a model with two fins positioned at 45° in relation to the longitudinal axis.

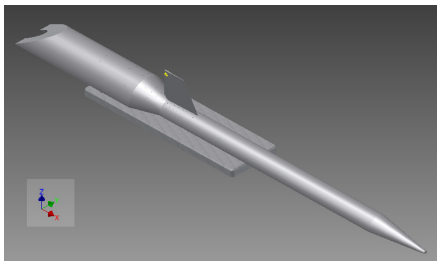

Fig. 3. The Sonda III half-model in the one-fin configuration.

Results from the test carried out with the no-fin configuration were discussed in [3]. The presence of expansion waves followed by a shock wave downstream of the frustum cone was experimentally observed. Numerical code using Computational Fluid Dynamics, CFD, reinforced the results.

In this paper we present experimental data related to the model in the one-fin configuration and analyse the influence of the fin downstream of the airflow. The model is in a scale 1:8 of the real vehicle.

The importance of this study is to characterise the airflow around the model to help in the design optimisation of vehicles developed by the Institute.

2. METHODOLOGY

Details of the wind tunnel tests are presented in section 2.1, the tested model in section 2.2, the mathematical modelling in section 2.3 and the numerical code in section 2.4.

2.1. Wind tunnel test

The airflow regimes covered by the wind tunnel tests range from Mach number 0.30 to 1.10. Only Mach number M = 0.90 is analysed in this extended abstract.

The TTP test section is 0.25 m high, 0.80 m long and 0.30 m wide and has longitudinally slotted walls to favor the uniformity of the airflow.

The measured airflow parameters are the local static pressure on the model surface, p, the freestream static pressure, p_∞, and the total pressure of the airflow, p_0. The mean and standard deviation of the temporal pressure signals are estimated.

The local pressure coefficient, $-C_P$, and the Mach number, M, are evaluated, as well as their associated uncertanties, u_{-C_P}, and u_M. The law of propagation of uncertainty was employed to estimate the uncertainty values [4].

2.2. The Sonda III model

The half model is a 1:8 scale of the real vehicle and has 154 pressure taps positioned at 22 stations along the fuselage, named A to V, classified from the first to the second stage. Each station is composed of 7 taps in a circumferential arrangement (Fig. 4).

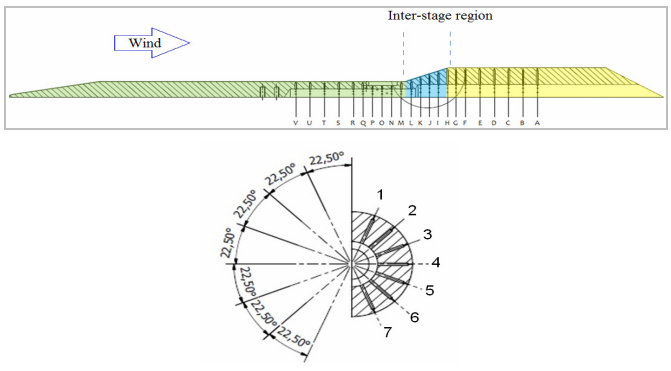

Fig. 4. Positioning of the pressure taps on the model surface and detail of each station.

The model is mounted in a flat platform which will be fixed to the lateral wall of the TTP wind tunnel test section (Figs. 5 and 6). Pressure taps are connected to pressure instrumentation throughout plastic tubing (Fig. 7).

The total length of the Sonda III half model is approximately 780 mm. The diameters of the first and second stages are around 70 and 37 mm, respectively. Both model and platform were made from Aluminum and the fin was made from steel.

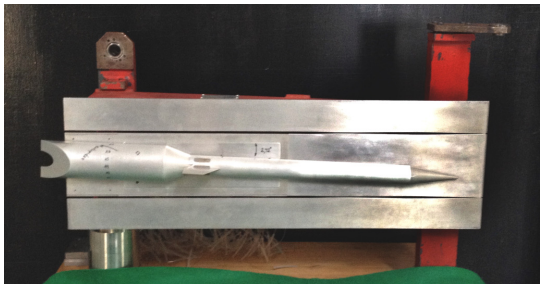

Fig. 5. Assembly model-platform.

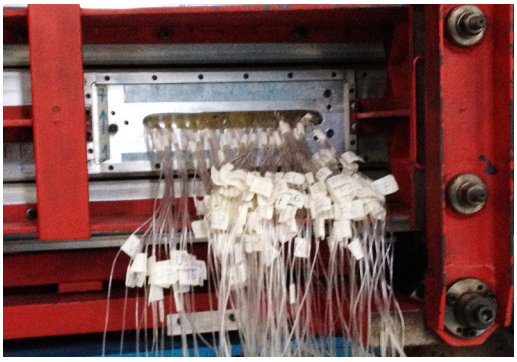

Fig. 6. The model fixed to the lateral wall of the TTP test section.

Fig. 7. Tubing for connection of the pressure taps to instrumentation.

2.3. Mathematical modelling

The pressure distribution on the model surface can be represented in terms of the pressure coefficient defined by [1]:

$$C_P \equiv \frac{p - p_\infty}{q_\infty} \tag{1}$$

where p is the local static pressure measured at each pressure tap station of the model, p_∞ is the freestream static pressure and q_∞ is the freestream dynamic pressure. The static pressure sensor used to measure p_∞ is positioned on the upper part of the wall at the beginning of the wind tunnel

test section. The freestream dynamic pressure, q_∞, is defined by:

$$q_\infty \equiv \frac{1}{2}\rho_\infty V_\infty^2 \tag{2}$$

where ρ_∞ and V_∞ are the freestream density and velocity, respectively.

In this study, the air is considered as a perfect gas. Its density is calculated by:

$$\rho_\infty = \frac{p_\infty}{RT_\infty} \tag{3}$$

p_∞: freestream pressure in pascal;
R: perfect gas constant, equal to 287 J/(kg.K) for normal air; and
T_∞: freestream temperature expressed in kelvin.

The airflow Mach number, M, is the ratio between velocity, V, and the speed of sound, a:

$$M = V/a \tag{4}$$

In equation (4), a represents the speed of sound travelling through the air, considered in this study as a perfect gas. Its value is estimated by:

$$a = \sqrt{\gamma RT} \tag{5}$$

where
T: temperature expressed in kelvin; and
γ: ratio of specific heats, equal to 1.4 for air considered as a perfect gas.

Rearranging equation (1) by using (2), (3), (4) and (5) results in:

$$-C_P = \frac{p_\infty - p}{\frac{1}{2}\gamma p_\infty M_\infty^2} \tag{6}$$

In regions of the flow where $p > p_\infty$, the pressure coefficient $-C_P$ will have a negative value.

Considering the flow in the test section as compressible flow, the freestream Mach number, *i. e.*, the Mach number at undisturbed condition (before reaching the model) is given by:

$$M_\infty^2 = \frac{2}{\gamma - 1}\left[\left(\frac{p_0}{p_\infty}\right)^{\frac{(\gamma-1)}{\gamma}} - 1\right] \tag{7}$$

where p_0 is the freestream total pressure.

As already mentioned, the static pressure tap p_∞ is located on the upper wall of the test section and is connected to a pressure sensor. The total pressure sensor used to measure p_0 is located in the stilling chamber of the circuitry.

The same expression is used to calculate the local Mach number, M. For simplification, the total pressure for the local Mach number is considered equal to the total pressure of the wind tunnel.

If we employ the law of propagation of uncertainty to (6) we obtain [4]:

$$u_{-C_p}^2 = \left(\frac{\partial C_p}{\partial p}\right)^2 u_p^2 + \left(\frac{\partial C_p}{\partial p_\infty}\right)^2 u_{p_\infty}^2 + \left(\frac{\partial C_p}{\partial M_\infty}\right)^2 u_{M_\infty}^2 \tag{8}$$

resulting in the estimation of the pressure coefficient uncertainty:

$$u_{-C_p}^2 = \left(\frac{-1}{\frac{\gamma}{2} p_\infty M_\infty^2}\right)^2 u_p^2 + \left(\frac{p}{\frac{\gamma}{2} p_\infty^2 M_\infty^2}\right)^2 u_{p_\infty}^2 + \left(\frac{2(p_\infty - p)}{\frac{\gamma}{2} p_\infty M_\infty^3}\right)^2 u_{M_\infty}^2 \tag{9}$$

2.4. The numerical code

The numerical code used to simulate the airflow was the CFD++®. The simulation was based on the Reynols-Averaged Navier-Stokes equations, RANS, in a three dimensional formulation. The Spalart-Allmaras one equation turbulence model was chosen [5]. The discretization scheme is based on finite volumes method in an unstructured mesh. An implicit time marching method associated with a multi-grid scheme was adopted.

The complete Sonda III model was simulated in free flight conditions, *i. e.*, the walls of the TTP test section were not considered. The computational mesh has a symmetrical plane crossing the centerline of the model, which coincides with the longitudinal base of the tested half model. The second stage fin of the vehicle is perpendicular to the symmetrical plane. The distance of the far field frontier is around 37 diameters of the first stage of the model. To provide a better capture of the boundary layer the mesh was refined near the model surface (Fig. 8). A 16% mesh stretching rate was adopted near the fuselage and the fin to save the number of calculation volumes and satisfy y+ condition of about 1, as required by the Spalart-Allmaras turbulence model. This results in 50 points within the boundary layer region.

The history of the maximum residue was monitored and the solution was considered converged after a decrease of four orders in magnitude. The simulation was undertaken in a parallel environment using 24 processors in a cluster of computers. The total convergence time for the solution was 15 hours.

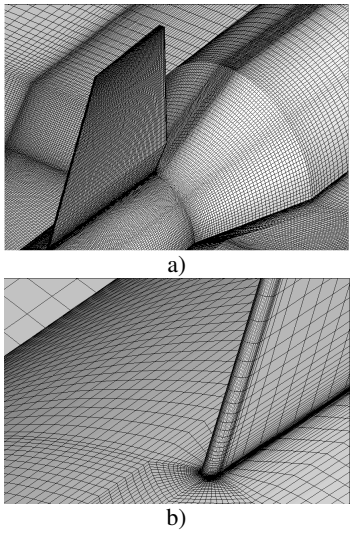

a) b)

Fig. 8. The Sonda III mesh. a) Inter-stage region. b) Detail of the leading edge of the fin.

3. RESULTS

The model under test is the Sonda III half model in the one-fin configuration. In this paper the results are related to the airflow velocity corresponding to nominal Mach number 0.90.

The Mach number distribution along the model surface is presented in Fig. 9. The uncertainty bars are also shown in Fig. 9. A schematic representation of the model is included in the picture in order to clarify the pressure tap positioning, as seen in Fig. 4. The results are related to 20 stations because pressure taps S and U were not considered due to limitations in the pressure instrumentation.

Following the wind direction, an abrupt increase in velocity occurs after the inter-stage region. This phenomenon was observed after pressure tap H, located at around 50 mm, where the airflow encounters a convex corner. At point G, the Mach number value M is greater than 1.

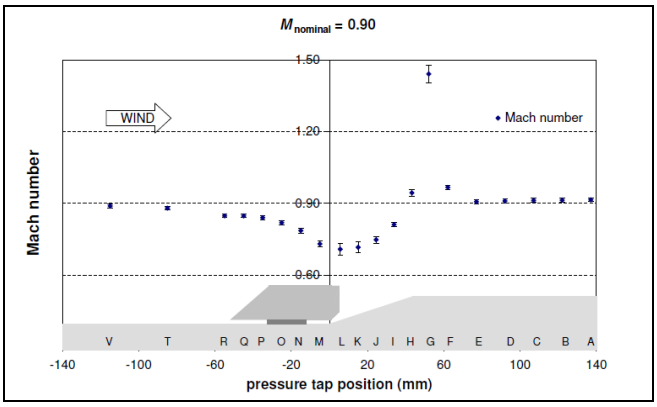

Fig. 9. Mach number distribution on the Sonda III surface.

The pressure coefficients, $-C_P$, at each individual pressure tap are presented in Fig. 10. For a better visualization, a three-dimensional representation of the same data is shown in Fig. 11. Data points were interpolated to construct the picture. Grid nodes represent measured points.

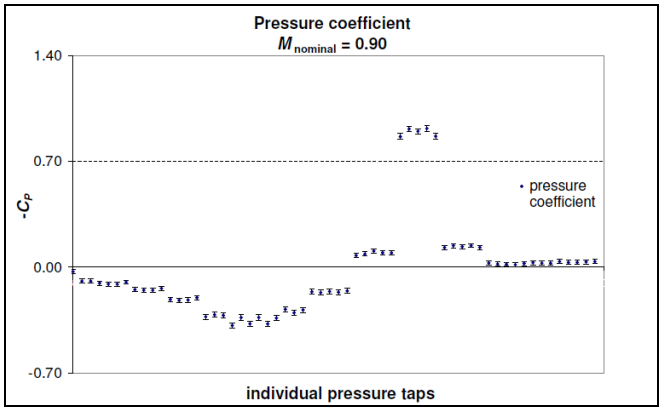

Fig. 10. Pressure coefficient at each pressure tap.

Pressure coefficients belonging to a particular station were grouped together and the mean and standard deviation values were estimated to compose Fig. 12. One can observe the contribution of the measurement variability of each pressure tap to the uncertainty u_{-C_P} at each station. This effect is more remarkable between 0 and 60 mm, downstream of the region where the fin of the model is located.

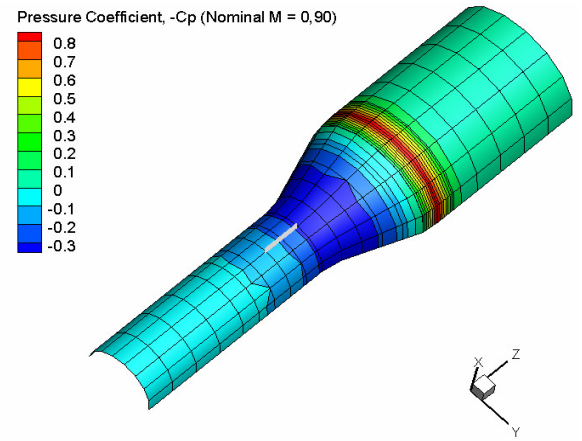

Fig. 11. Same data as in Fig. 10.

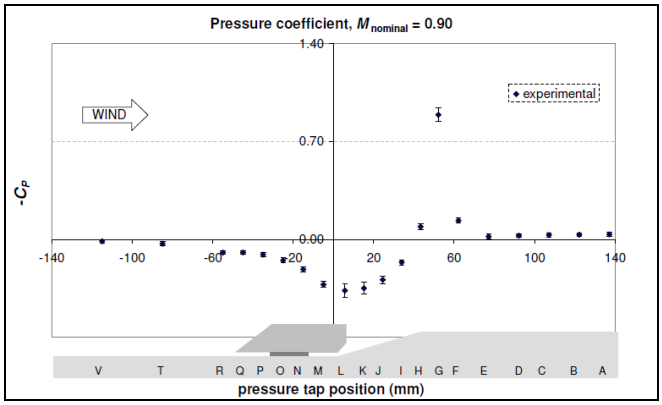

Fig.12. Pressure coefficient at the pressure stations.

Figure 13 compares the pressure coefficients obtained in the tests of the model with and without fins. As expected, no significant differences were found because the fin is a slender body, but some disagreement was observed in the region between -60 and 0 mm due to disturbances at the pressure stations corresponding to the fin length.

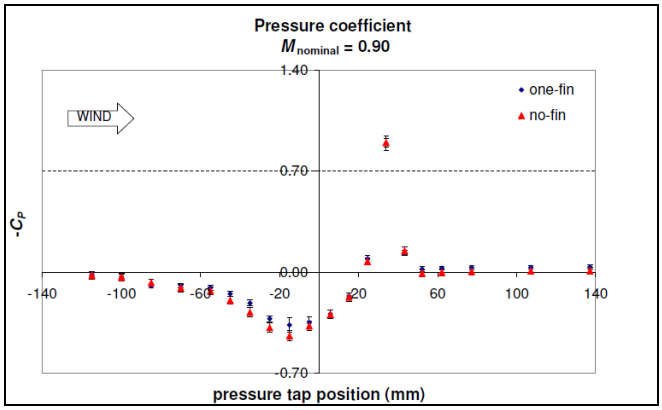

Fig. 13. Pressure coefficient comparison for two different Sonda III configurations: one-fin and no-fin.

The increase in $-C_P$ after the frustum cone reveals the presence of expansion waves. The difference $(p_\infty - p)$ between the freestream static pressure and the local static pressure in

(6) becomes more positive and $-C_P$ achieves its maximum value at pressure tap G. The drop in $-C_P$ downstream of pressure tap G was caused by the presence of a shock wave.

To better understand the aerodynamic phenomena taking place in the airflow, Computational Fluid Dynamics, CFD, was used. In Fig. 14, the freestream static pressure p_∞ is equal to 53,323 Pa. The CFD data are related to the 0^o direction, coincident with pressure taps number 4 (see Fig. 4). The convex corner at the end of the frustum cone causes a decrease in the local static pressure p and the local Mach number M increases, as shown in Fig. 15. The airflow recovers the freestream condition through the presence of a shock wave.

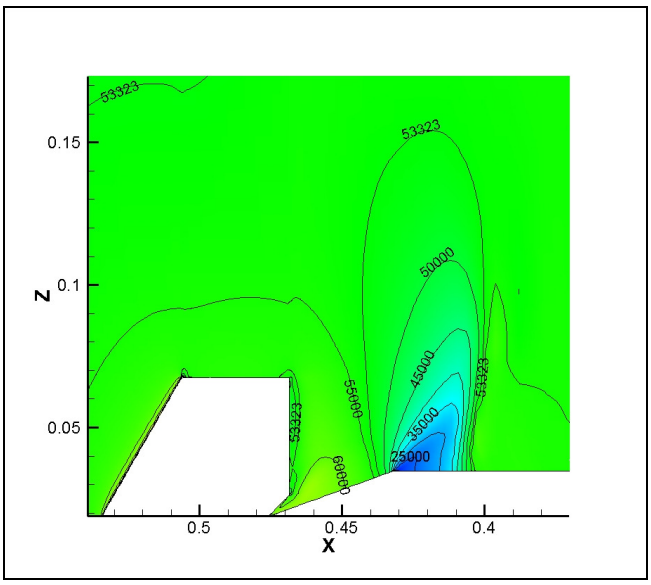

Fig. 14. The static pressure, p, in the flow field around the inter-stage region. The freestream static pressure is 53,323 Pa.

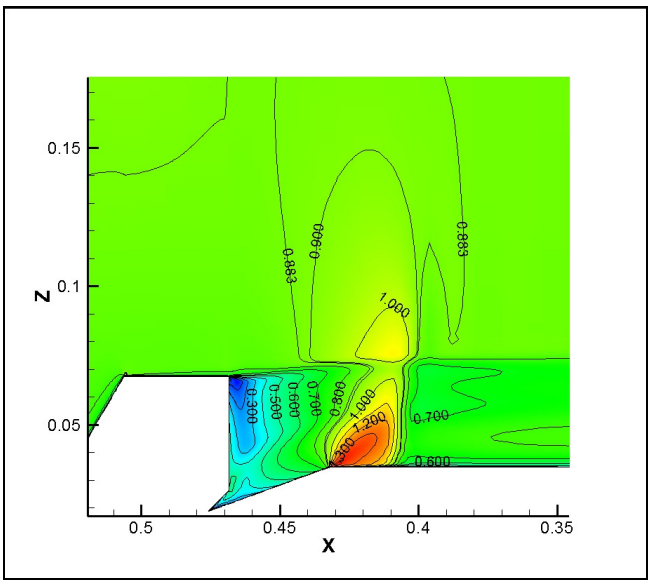

Fig. 15. The Mach number, M, in the flow field around the inter-stage region. The freestream Mach number is 0.883.

Figure 16 depicts a Schlieren image in which both phenomena are shown: expansion and shock waves. The Sonda III model used for this shot is a complete model configuration in a 1:20 scale of the actual size of the vehicle. Flow direction is from left to right.

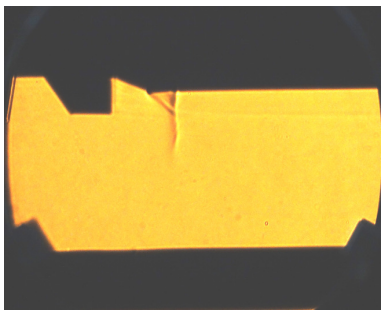

Fig. 16. Schlieren image of expansion waves followed by a shock wave downstream of the frustum cone.

A comparison between the pressure coefficient distribution obtained by using CFD and experimental data is shown in Fig. 17. Results do not fully agree but the information supplied by each method is complementary. The major difference is the location where the shock wave occurs. A more precise investigation is necessary to understand this discrepancy. A possible cause is that a relaminarisation of the boundary layer on the model surface is present in the experiment.

The $-C_P$ value decreases in two steps in the simulation data. It is not possible to know if this behavior occurs in experimental data due to restrictions in the number of pressure taps. To overcome this limitation, a test employing Pressure Sensitive Paint, PSP, will be conducted in future investigations. Also, visualization techniques such as Laser Doppler Velocimetry, LDV, may be used to analyse the boundary layer condition on the model surface.

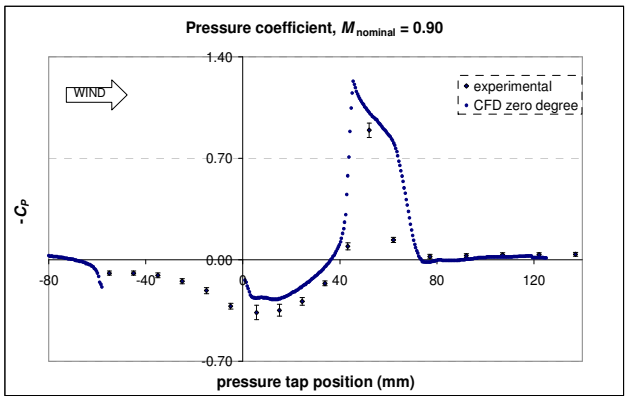

Fig. 17. Experimental and CFD results.

4. CONCLUSIONS

The airflow properties around the Sonda III vehicle are being analysed by testing a half model in a transonic wind tunnel. Mach number, pressure coefficient and associated uncertainties are estimated in order to detect disturbances caused by aerodynamic phenomena which can affect the flight performance. The results presented in this paper are related to the half model with one fin. Previous tests with a no-fin configuration were carried out in the first phase of the campaign. It was shown that the presence of the fin does not cause significant differences in the pressure distribution coefficient on the model surface. Numerical simulation employing CFD complements the experimental

investigation. The study revealed the presence of shock and expansion waves in the first stage of the vehicle, after the inter-stage region. The simulation and experimental data differ in this region. The CFD simulation showed that there is an aerodynamic phenomenon in the airflow that the experimental technique employed in the wind tunnel tests was not able to capture. Further studies are being planned in order to explain the differences. The first of them is to carry out tests employing methods which overcome the spatial limitation of the pressure taps. Investigation of the boundary layer condition on the model surface with flow visualization techniques is also planned. Once the information is supplied by the supplementary experiments, it will be sent to the CFD team for simulation refinement with updated airflow conditions.

ACKNOWLEDGMENTS

The authors would like to express their gratitude to CNPq, the Brazilian Counsel of Research and Development for their help during the development of this study through grant 560200/2010-2 and the individual support number 156381/2014-1. The simulation study is supported by CEPID/FAPESP 2013/07375-0.

REFERENCES

[1] J. Anderson Jr., Fundamentals of Aerodynamics, Mc Graw Hill, New York, 2007.

[2] M. L. C. C. Reis, J. B. P. Falcão Filho, M. C. C. Araújo, "Uncertantiy in airflow field parameters in a study of shock waves on flat plate in transonic wind tunnel", *Journal of Physics*, Conference Series (Print), vol. 459, p.012034, 2013.

[3] M. L. C. C. Reis, J. B. P. Falcão Filho, E. Basso, V. R. Caldas, "Pressure coefficient evaluation on the surface of the Sonda III model tested in the TTP Pilot Transonic Wind Tunnel", *IMEKO Joint Symposium TC1-TC7-TC13*, Madeira, Portugal, Sept. 2014.

[4] BIPM/JCGM 100:2008, Evaluation of measurement data – Guide to the expression of uncertainty in measurement (GUM 1995 with minor corrections), 2008.

[5] D. C. Wilcox, *Turbulence modeling for CFD*, 2.Ed. La Cañada: DCW Industries, 1998.